

Charm in cosmic rays
(The long-flying component of EAS cores)

I.M. Dremin¹, V.I. Yakovlev²
Lebedev Physical Institute RAS, 119991 Moscow, Russia

Abstract

Experimental data on cosmic ray cascades with enlarged attenuation lengths (Tien-Shan effect) are presented and analyzed in terms of charm hadroproduction. The very first estimates of charm hadroproduction cross sections from experimental data at high energies are confirmed and compared with recent accelerator results.

1 Introduction and brief overview

Charm was found in cosmic rays in 1971 by Niu et al [1] (no such name was ascribed to it at that time). The creation of charm particles provoked in 1975 to relate them [2] to the long-flying component of the cores of extensive air showers (EAS) observed a couple of years before [3, 4] and named as the Tien-Shan effect. This idea was however abandoned for several years because no precise data on properties of charm hadrons existed. Let us note that the similar elongation of the cascades observed at Aragatz installation in Caucases with rather low statistics was analyzed in late 1970s in [5] but the resulting estimates of particle parameters (mass about 10 GeV and lifetime 10^{-10} s) were misleading.

Open charm measurements in accelerator experiments date back to late 1970s when D and \bar{D} mesons were first detected. In earlier 1980s, the leading effect in Λ_c production was declared by experimentalists [6, 7] and supported by theorists [8]. The small inelasticity coefficient for Λ_c was also advocated [8, 9]. The spectra of D -mesons were considered to be much softer than those of Λ_c [7, 10]. The charm hadroproduction cross sections measured at energies $\sqrt{s} < 20$ GeV were quite small (less or about $10 \mu b$). It looked improbable that they increase fast with energy even though first calculations in the quark-gluon strings model showed [11] that they can become as large as 0.1 - 1 mb at energies exceeding $\sqrt{s} = 100$ GeV. Smaller values were however obtained in [12].

Meantime, masses and lifetimes of charm particles were measured more and more accurately. In parallel, the more precise data about the long-flying component of the EAS cores were obtained [13]. The specific structure in the energy dependence of the attenuation length of cascades observed in the hadron calorimeter [14, 15] revived the idea about charm production responsible for these peculiar features [16]. The starting impact was related with long lifetimes of charm particles. Both analytical and computer calculations with kinetic equations [17] and Monte-Carlo simulations of cascades in the calorimeter [18, 19, 20] were attempted. They lead to the conclusion [16, 18, 21] that the charm production cross section can be as large as 1.4 - 2.8 mb at the laboratory energy $E_L = 10 - 20$ TeV ($\sqrt{s} = 140 - 200$ GeV) and about 3 - 5 mb at $E_L \approx 100$ TeV ($\sqrt{s} \approx 450$ GeV). These estimates were the earliest values for the charm hadroproduction cross sections obtained from experimental results at very high energies. The cosmic

¹e-mail: dremin@lpi.ru

²e-mail: yakovlev@sci.lebedev.ru

ray data obtained with lead and X-ray emulsion detectors also showed the existence of the long-flying cascades [22]. Later it was concluded [23, 24] that they support a large charm cross section at $\sqrt{s} = 300$ GeV. These values of the charm hadroproduction cross section were considered as being extremely large until recent experiments at RHIC energy $\sqrt{s} = 200$ GeV claimed (see, e.g., [25]) that this cross section per nucleon in pp and d-Au collisions is $1.4 \pm 0.2 \pm 0.4$ mb according to STAR collaboration [26, 27] and $0.92 \pm 0.15 \pm 0.54$ mb according to PHENIX collaboration [28]. The same collaborations extracted the same cross sections from Au-Au collisions at $\sqrt{s} = 200$ GeV and give the following numbers: $1.11 \pm 0.08 \pm 0.42$ mb for STAR [29] and $0.622 \pm 0.057 \pm 0.160$ mb for PHENIX. The compilation of both accelerator and cosmic ray data on charm hadroproduction cross section at various energies is demonstrated in Fig. 1.

The difference by a factor about 1.5 - 2 between the two collaborations at RHIC is related to problems in extracting the cross section values. They are obtained from a finite number of measured D mesons in a particular decay channels by using many correction factors. Especially important are the extrapolations to the full phase space because of undetected forward region and the role of other numerous unmeasured charm hadrons. Let us stress here that namely forward region is crucial in cosmic ray experiments.

The situation with QCD calculations is also not clear yet even though there has been a great deal of improvement over last 10-15 years. In 1990s they predicted rather low values of these cross sections with a very mild increase with energy. Recent results taking into account higher order (NLO) perturbative corrections [30, 31] give larger values and improve the situation. They are however still lower by a factor 5-6 than STAR data. The quark-gluon strings model is in a better position (see, e.g., [32, 33]) predicting larger cross sections. The heavy quark production was also considered in the semihard QCD approach [34].

In view of this intriguing and rapidly evolving situation we decided to reanalyze previous cosmic ray data and compare with results obtained during last years.

Let us mention that the charm particle production is also important for muon studies, both underground and in gamma-astronomy [35, 36].

2 Qualitative expectations

Before discussing the experimental installation in detail, we would like to explain the physics of the phenomenon and present the qualitative expectations which gave rise to the idea about the role of charm particles. EAS cores consist of beams of high energy hadrons. These hadrons interact actively when they pass through the dense matter of the calorimeter. Most interactions give rise to abundant pion production. These pions create new pions in inelastic collisions. The hadronic shower is developed with the typical attenuation length in lead about 600 - 700 g/cm². In some events the charm particles are however produced. Their decay lengths are of the order of tens or hundreds μm at comparatively low energies. Thus the low energy charm particles decay within the main shower and nothing special happens. The decay length is proportional to the γ -factor. Therefore, high energy charm particles are able to penetrate to larger depths in the calorimeter. If they carry large portion of initial energy, then the shower elongates and the attenuation length increases. However, at a somewhat higher energy it can happen

that a produced charm particle passes through the whole calorimeter without decay. Its energy is no more detected in the calorimeter. The attenuation length should come back to its standard values. Thus one would expect to observe a maximum in the energy dependence of the attenuation length.

Let us advertize in Fig. 2 the final result of the Tien-Shan experiment where the observed energy dependence of the attenuation length of hadronic showers in EAS cores is plotted. This anticipates its detailed discussion below. The upper and lower experimental points correspond to two classes of cascades separated according to special methods among the available amount of data.

We will interpret the upper points as typical for long-flying cascades with decaying high energy particles because they are obtained from samples enriched by such particles as advocated below. With three peaks in it, one is tempted to ascribe this plot to D^\pm , D^0 and Λ_c . The decay length l_i for any species i is given by

$$l_i = c\tau_i\gamma_i = c\tau_i\frac{E_i}{m_i}, \quad (1)$$

where τ_i is its lifetime, γ_i is the γ -factor, E_i , m_i are its energy and mass. If the interaction with production of a charm particle took place in the upper part of the calorimeter, then the attenuation length would return to its standard value at $l_i = z_c/\rho$ where z_c is the calorimeter depth in g/cm² and ρ its average density in g/cm³. Then all particles with energies exceeding

$$E_i = \frac{m_i z_c}{c\tau_i \rho} \quad (2)$$

slip down the calorimeter and decay outside it.

Thus the peak can be ascribed only to those particles whose energies are high enough to decay at lengths larger than 0.3 - 0.5 m and lower than E_i (2). Its shape and height are determined by the energy behaviour of charm hadroproduction cross section which favours higher energies and drives the peak to (2). For the parameters of Tien-Shan calorimeter $z_c = 850$ g/cm², $\rho = 3.54$ g/cm³, i.e., $z_c/\rho = 240$ cm, and particle masses and decay lengths $m_{D^\pm} = 1869$ MeV, $m_{D^0} = 1864.6$ MeV, $m_{\Lambda_c} = 2284.9$ MeV, $c\tau_{D^\pm} = 311.8$ μ m, $c\tau_{D^0} = 123$ μ m, $c\tau_{\Lambda_c} = 59.9$ μ m one gets $E_{D^\pm} = 14.4$ TeV, $E_{D^0} = 36.4$ TeV, $E_{\Lambda_c} = 91$ TeV. It follows that the initial energies should be high enough for such particles to be created³. They can be estimated by dividing the above numbers by the Feynman ratios $x_i = E_i/E_0$. Qualitatively we can say that the values of $\langle x_i \rangle \approx 0.2 - 0.3$ would correspond to peaks positions in Fig. 2. The ratios of energies at which peaks are positioned in Fig. 2 correspond quite well to the ratios of energies of various charm particles. Thus these findings favour the hypothesis about charm particles initiating the effect of elongated cascades.

This is however an oversimplified estimate. Beside knowing the spectra of charm particles, i.e., x_i -distributions, one should use the energy and atomic number dependence of the charm production cross section on nuclei, the cross section of the interaction of a particular charm particle in a medium and its inelasticity coefficient, i.e., the share of energy spent by it in interactions with the calorimeter matter. The primary spectrum and composition of cosmic rays as well as the secondary interactions in the cascade must

³The Λ_c lifetime estimated in [1] was about 18 times less. Therefore it required in initial estimates [2] too high energies that prevented further work on this hypothesis.

be taken into account as well. Also, one should know at which depth in the calorimeter the charm particle was produced because in the proper estimate for E_i the value z_c should be replaced by $z_c - z_1$ where z_1 is just this depth. After all these factors are accounted in Monte-Carlo simulations, the results and their sensitivity to various parameters can be quantitatively studied. Nevertheless, one can start the next stage of qualitative approximations with analytical approach using the simplified kinetic equations. Before doing this we describe in more details the experimental installation and methods of analyzing experimental data.

3 Experimental installation

Extensive air showers (EAS) were registered in the ionization calorimeter placed in the Tien-Shan mountains at the altitude 3330 m. It consists of the lead absorber and ionization chambers of the total area of 36 m² and the height 2.4 m. The total thickness of the lead absorber (including some other elements recalculated to lead) is 850 g/cm². There are 17 rows of 48 copper ionization chambers with size 5.5·24·300 cm³. Each chamber has its own analogue digital convertor (ADC) with the dynamical range 2·10⁴. The accuracy of signal measuring is better than 10% in the whole range. Signals from the chambers are stored in the diode-capacitor cells. Then the series of pulses is sent to all ADC inputs. Each subsequent pulse is 10% higher than the previous one. If the height of the pulse exceeds those stored by 10%, its number n is fixed. Thus all ADC are calibrated after each trigger. The information is stored in magnetic tapes.

The operation control of the calorimeter includes the everyday statistical analysis of each channel. The statistics in individual ionization chamber is compared with the average statistics in each particular row.

4 Methods of analysis of long-flying cascades

The shower array selects EAS with the number of particles exceeding 1.3·10⁵. Then the EAS cores which do not cross the calorimeter sides were selected for analysis.

In Fig. 3 we demonstrate an averaged cascade at the energy 37.6 TeV. The averaging has been done over 765 events. It is clearly seen that the electron-photon component of EAS dominates at the depths less than 133 g/cm². Therefore, the energy of the hadronic component has been estimated by the energy released in the calorimeter at the depths from 133 to 850 g/cm². The events are selected according to this value.

The ionization curves of the averaged cascades are approximated by the exponential function $\exp(-z/L)$ in the depths interval 344 - 850 g/cm² (see Fig. 3) and the attenuation length L is calculated. Its mean value is estimated both by simple averaging and from the distribution of inverse values $1/L$ in individual cascades. Even though the difference between these estimates is small, their average value is chosen for further analysis. Its energy dependence has been found in two runs of measurements (with statistics 6976 and 3617 events at energies higher than 3 TeV) done in the 6 years interval. The results fully coincide that proves the stability of the calorimeter operation. Also, the position of the absolute cascade maximum is determined. It has been shown that it is directly correlated with the energy dependence of the attenuation length.

Moreover, it was attempted to find how the energy is distributed around the cascade axis at different energies. For this purpose, the ratio $C(z)$ of the ionization energy released within the circle with the radius 36 cm around the axis in the row of chambers at some depth z to the total energy in all chambers of the same row has been measured. This method of analysis is crucial for separation of cascades with charm particles from the standard cascades.

5 Results

The most spectacular feature of the attenuation lengths energy dependence is their increase from values about 900 g/cm² at 20 TeV to about 1500 g/cm² at energies close to 100 TeV and 1900 g/cm² at 300 TeV with their decrease at even higher energies as seen in Fig. 2⁴. This increase is shown to be related to the shift of the absolute cascade maximum to larger depths with increase of the attenuation length (or energy) as demonstrated in Table 1.

Table 1

The position of the absolute cascade maximum z_m at different attenuation lengths L .

| $z_m, \text{g/cm}^2$ | $L, \text{g/cm}^2$ |
|----------------------|--------------------|
| 374 | 667 ± 15 |
| 600 | 847 ± 60 |
| > 600 | 2196 ± 260 |

If this maximum is attributed to the decay products of a high energy particle, it shows that this particle penetrates to larger depths in the calorimeter at higher energies as one would expect for a particle with a fixed and rather large lifetime.

Further insight in the problem which helped reveal the fine structure of this increase seen in Fig. 2 was obtained from studies of the concentration behaviour. Its values have been measured for cascades with different attenuation lengths. The dependence of the concentration $C(z)$ on the depth z was approximated by the simple linear line $C(z) = a + bz$. Actually, it has been observed that b depends on the attenuation length as shown in Fig. 4. Its average value at low attenuation lengths $L < 800 \text{ g/cm}^2$ is negative $b_{low} = -1.15 \cdot 10^{-4} \text{ cm}^2/\text{g}$ but it is positive at large attenuation lengths $L > 800 \text{ g/cm}^2$ ($b_{large} = 1.4 \cdot 10^{-4} \text{ cm}^2/\text{g}$). This demonstrates that at low energies the cascade energy spreads from the center while at large energies it tends to be more concentrated near it. The strongly attenuated cascades have a relatively large transfer into their peripheral region, whereas the long-flying cascades show increasingly more ionization concentration at larger depth values in their core region. This could be understood by the conjecture that energetic long-lived unstable particles are produced in the long-range cascades. The same feature is confirmed by the difference in the dependence of the positions of the absolute cascade maximum (Fig. 5) on the absorber depth. For $L < 800 \text{ g/cm}^2$ they decrease faster than for $L > 800 \text{ g/cm}^2$: the exponents differ by the factor about 2.5.

⁴The fine structure of this dependence is discussed below

These findings allowed to plot separately the energy dependences of $L(E)$ for cascades with $b > 0$ and $b < 0$. The most remarkable difference between the two new cascade subsamples appears in the energy dependence of the attenuation length (Fig. 2). For the cascades with the negative sign of b the data are compatible with the usual rather mild dependence shown by the lower dots in Fig. 2 typical of single nucleon cascades containing only pions. This gives a confidence that the proposed selection criterion according to the sign of b properly separates the standard cascades. As to the subsample of cascades with the positive values of b , which is expected to be enriched with cascades containing the long-lived unstable particles, the irregular behaviour with pronounced maxima is observed (the upper dots in Fig. 2). All this favours the hypothesis that the decaying particle is the leading one in the production process. It plays more important role at high energies and releases its energy close to the shower axis.

The sign of b has been used for estimates of the total cross section of charm hadroproduction. The individual cascades with energies higher than 10 TeV were separated according to the sign of b . It happened that they were split into two equal groups. The distributions of their attenuation lengths were obtained. The cascades with positive b are shifted to larger depths than those with negative b (see Fig. 6). If this excess is attributed to charm production then one would get for the charm production cross section per nucleon σ_c :

$$\sigma_c = (0.16 \pm 0.023)\sigma_{pPb}/A_{Pb}. \quad (3)$$

Here it is assumed that due to smallness of σ_c the cross section of charm hadroproduction on lead is proportional to the atomic number that is accounted by the rightmost factor $A_{Pb} = 207$. Another method of σ_c estimate is based on the experimental fact that some part (0.358) of cascades with the attenuation length less than 800 g/cm² have positive b . If this is ascribed to fluctuations in usual cascades without charm particles then

$$\sigma_c = 0.5(1 - 0.358)\sigma_{pPb}/A_{Pb} = (0.321 \pm 0.072)\sigma_{pPb}/A_{Pb}. \quad (4)$$

Thus the charm production cross section per nucleon was estimated [15, 21] as $\sigma_c=1.4 - 2.8$ mb at energies 10 - 20 TeV. This is the very first estimate of the charm hadroproduction cross section from experimental data at very high energies. Nowadays accelerator results are close to these findings as discussed above (see Fig. 1).

6 Theoretical interpretation

6.1 Analytical and computer solutions of the kinetic equations

First, it was attempted to show by simple analytical means that production of the long-lived particles can give rise to the increase of the attenuation length with its subsequent decrease for those showers with increasingly high energies in which the charm particle escapes from installation before decay. The simplified system of the kinetic equations consisted of three equation taking into account the evolution of the charm (c), nucleon (N) and pion (π^\pm) components:

$$\frac{dS_c}{dz} = -\gamma S_c,$$

$$\begin{aligned}\frac{dS_N}{dz} &= -\beta S_N + \delta S_c, \\ \frac{dS_{\pi^\pm}}{dz} &= -\alpha S_{\pi^\pm} + \frac{2}{3}\beta S_N + \frac{2}{3}(\gamma - \delta)S_c\end{aligned}\quad (5)$$

with the initial conditions

$$\begin{aligned}S_c(0) &= \frac{\sigma_c}{\sigma_t}\langle x_c \rangle, \\ S_N(0) &= 1 - K_N, \\ S_{\pi^\pm}(0) &= \frac{2}{3}\left(K_N - \frac{\sigma_c}{\sigma_t}\langle x_c \rangle\right).\end{aligned}\quad (6)$$

Here S means the share of initial energy taken by the charm, nucleon and pion components, z is the depth along the cascade axis, σ_c/σ_t is the probability of the charm particle creation. A single species of charm particles is considered here.

The coefficients in the equations are

$$\alpha = \frac{1/3}{\lambda_\pi}, \quad \beta = \frac{K_N}{\lambda_N}, \quad \gamma = \frac{1}{\lambda_d} + \frac{K_c}{\lambda_c}, \quad \delta = \frac{1 - B}{\lambda_d},\quad (7)$$

where λ_i , K_i are the interaction lengths and inelasticity coefficients of the corresponding component, λ_d is the decay length of the charm component, B is the share of energy of pions in the decay of the charm particle to nucleon and pions.

This system has been solved. Here we however demonstrate only the qualitative features of the solution for the pion component energy with a particular choice $B = 1$, $K_N = 1$ because it can be written in the simple analytical form as

$$\frac{3}{2}S_{\pi^\pm} = e^{-\alpha z} + \frac{\sigma_c}{\sigma_t} \frac{\langle x_c \rangle}{\gamma - \alpha} [\alpha e^{\alpha z} - \gamma e^{-\gamma z}].\quad (8)$$

The formula (8) clearly shows that the production of charm particles leads to a slight "deepening" in the cascade ionization curve (due to the term with the negative sign in the brackets) which, at higher energies, is replaced by the "hump" with a subsequent exponential decrease at larger depths. This is the origin of the humps in the energy dependence of attenuation lengths.

After establishing the main qualitative feature in the behaviour of attenuation lengths with the help of the simplified analytical approach the more rigorous computer solutions of kinetic equations were attempted. The system of kinetic equations looked like

$$\left(\frac{d}{dz} + \frac{1}{\lambda_i} + \frac{m_i}{E\tau_i c\rho}\right) F_i(E, z) = \sum_j \frac{1}{\lambda_j} \int_E^{E_0} F_j(E', z) W_0(E, E') dE' + \sum_j R_{ij}\quad (9)$$

for the energy distribution functions $F_i(E, z)$ of particles i at the depth z . The outflow of particles i due to interactions (λ_i) and decay (τ_i) is compensated by their production in inelastic interactions of particles j (W_{ij}) and in decays (R_{ij}).

Now four components were considered: both Λ_c and D -mesons were taken as charm particles. No accurate data about their lifetimes existed at the time when these calculations had been done. Therefore, the lifetime of Λ_c varied from $1.7 \cdot 10^{-13}$ s to $3.5 \cdot 10^{-13}$ s and

the average "D"-lifetime was chosen as $6.3 \cdot 10^{-13}$ s. The pion spectra were taken according to the standard CKP-prescription with the experimentally known energy dependence of the mean multiplicity. The spectrum of produced Λ_c was very hard, independent on x , i.e., $\langle x_{\Lambda_c} \rangle = 0.5$ [6, 7, 8]. This is in charge for large γ -factors of Λ_c , i.e., for large decay lengths. The D -spectrum was softer [9, 10] decreasing with x as $1 - x$ but somewhat harder in the case of primary pions to account for the leading effect. The interaction lengths were taken according to the additive quark model, i.e., they are almost equal for pions and Λ_c , 1.5 times larger for nucleons and about twice smaller for D -mesons. The inelasticity coefficients were put equal to $K_N = 0.63$ [37], $K_{\pi^\pm} = 0.7$ [37], $K_c = 0.1$ [8, 9]. The small inelasticity coefficient for Λ_c is crucial for their penetration to larger depths compared to pions. Thus, the three factors of interaction cross sections, decay lengths and inelasticity coefficients determine mostly the increase of the attenuation lengths. Electron-photon cascades due to decays of neutral pions were treated by common standards. The energy dependence of the charm production cross section was chosen so that it went through the experimental data at low ISR+FNAL energies (see Fig. 1) increasing to some constant values at very high energies. Its atomic number dependence was linear.

The equations were solved with the initial conditions $F_i(0, E) = W_{iN}(E, E_0)$, i.e. with all cascades initiated at the same point in the calorimeter. The exponential fit of the behaviour of the cascade ionization with the distance in the calorimeter at the depths from 344 to 800 g/cm² shows the energy dependence of the attenuation lengths. It is depicted in Fig. 7 for variants with high energy charm hadroproduction cross sections saturated at 2, 5, 10 mb at (and above) 100 TeV. The lines are marked by the corresponding numbers.

If compared with experimentally measured values of attenuation lengths, the charm cross section about 5 mb would be preferred. However the peak is shifted to somewhat larger energies. It appears at proper position only in Monte Carlo simulations taking into account the origin points of the individual cascades and the correct estimation of energy released in the calorimeter. The results for the standard cascade without charm production are shown by the dashed line. They are surely much below experimental data for all cascades but agree well with the lower dots in Fig. 2 obtained for cascades with $b < 0$.

Again, the qualitative effect of the increase and maximum in the energy behaviour of attenuation lengths due to charm production has been demonstrated. However, a single maximum appeared because, first, the two species of D -mesons were averaged with their lifetime chosen much closer to the Λ_c lifetime compared to present values and, second, no separation of cascades according to the sign of b was attempted. The very first interaction was always chosen at the top of the calorimeter. No account of the energy spectrum and primary composition of cosmic rays was done. In principle, all these deficiencies can be cured by the proper Monte Carlo simulations.

6.2 Monte Carlo simulations

In the more detailed Monte Carlo cascade simulations [18, 19, 20] some (but not all) of the above deficiencies were avoided. The positions of first interactions and values of energy release in the calorimeter were properly accounted. This has lead to better agreement with the energy locations of the maxima. Moreover, the structure appeared compared to Fig. 7. Unfortunately, the charged and neutral D -mesons were again considered together even

though it was taken into account that the lifetimes of Λ_c and D -mesons differ stronger than those values which were adopted above. This has also led to some structure in the maximum of the attenuation lengths as shown by dots in Fig. 8. It reflects quite well the corresponding structure in experimental data (shown by crosses in Fig. 8) if no separation of cascades according to the sign of b is done. The cascade simulation was performed for the energy region from 3 to 1000 TeV in intervals of $\Delta \log E=0.2$ with an integral spectrum of primary cosmic ray hadrons of a power law behaviour with an exponent equal to 1.8. For each step of $\Delta \log E$ a statistics of between 800 and 1600 cascades was required. Charm production was only included for energies exceeding 300 GeV, below which only standard cascades were allowed. The atomic number dependence was slightly modified to take into account the screening in case of larger charm cross section by replacing the linear dependence by $A^{1-\sigma_c/120mb}$ which is really insignificant for small σ_c . From these calculations and their comparison with experiment the value of the charm hadroproduction cross section was estimated [16, 18] as 3 - 5 mb at energies about 100 TeV (see Fig. 1).

Unfortunately, Monte Carlo cascades were not separated according to the sign of b . Namely this method has led to three peaks in Fig. 2. Thus, we can not claim that the structure seen in Fig. 2 has been quantitatively described, even though Fig. 8 points in this direction. Nevertheless, the successful description of the unseparated cascades is clearly seen. We conclude that at least qualitatively the specific structure in the energy behaviour of attenuation lengths has been understood.

7 Conclusions and perspectives

The long-flying cascades in the cores of extensive air showers have been observed experimentally and explained theoretically as a result of charm production at high energies. The peculiar structure in the energy dependence of the attenuation lengths has been ascribed to different species of charm particles possessing different lifetimes and masses.

There are several factors which determine the increase of the attenuation lengths. Charm particles are able to penetrate to large depths because they are rather heavy and spend less energy in inelastic collisions (small inelasticity coefficients). Also, this is in charge of the leading effect at their production and smaller interaction cross sections.

The main outcome of the analysis is the prediction of quite large cross sections for charm production which was done long before the accelerator data at high energies became available. These values looked suspiciously high if compared to the data at lower energies. Now they are however confirmed by recent experimental results of RHIC.

In view of better nowadays knowledge of the parameters of charm particles and good progress in developing the models of charm hadroproduction, the next step in refining theoretical results is foreseen. Both improved Monte Carlo simulations taking into account these developments and analysis of the simulated cascades by separating them into subgroups with the positive and negative signs of their concentration near the cascade axis can be done. The quantitative description of the three-maxima structure in Fig. 2 is the main goal. This is especially important for understanding the energy spectra of charm particles and more accurate estimates of their hadroproduction cross sections.

Charm particle decay can be important for EAS evolution in the atmosphere. It was

pointed out in [9] that the decay length of the charm particles becomes comparable with the vertical size of the atmosphere at energies $(1 - 7) \cdot 10^{17}$ eV. Recently it was shown [38] that the excess of EAS detected by AGASA installation [39] at energies above the GZK cutoff can be related with the increasing role of charm particles. There exist some other observations which could favour this interpretation. First, there is a strong excess [40, 41] of showers with energies above 10^{18} eV at large zenith angles ($> 60^\circ$). Second, experiments at Pierre Auger Observatory Surface Array revealed that "a significant number of very horizontal events are detected, offering a novel view of EAS" [42].

The experiment for confirming the crucial role of charm particles for hadronic cascades was proposed in [43]. The calorimeter with an air gap about 2.5 m should be used. Then the charm particles with energies less than 70 TeV, produced in the upper rows of the calorimeter, decay inside this air gap. That would intensify the energy release in the upper rows of the lower part of the calorimeter, i.e., lead to a hump in the energy distribution. The analogous experiment was proposed [44] with X-ray films. Such experiment is under way in Tien Shan station of LPI now.

Acknowledgements

This work has been supported in part by the RFBR grants 03-02-16134, 04-02-16320, 04-02-16445, NSH-1936.2003.2.

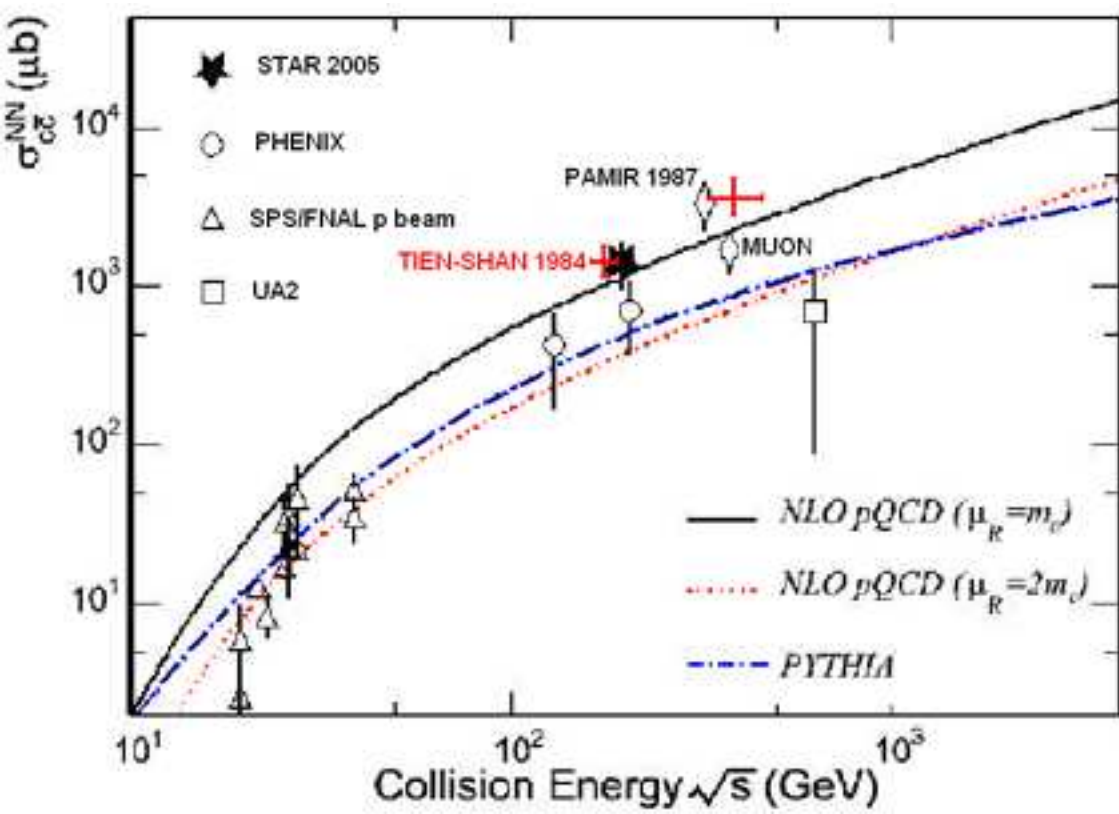
Figure captions.

- Fig. 1. The compilation of the charm hadroproduction cross sections at different energies from accelerator and cosmic ray data.
- Fig. 2. The attenuation length distributions for cascades with opposite signs of the derivative of the concentration b . The low-lying points correspond to the "standard" cascades with $b < 0$. The upper points are due to the long-flying cascades with $b > 0$, enriched by charm particles. The three-maxima structure is clearly seen.
- Fig. 3. The cascade at the energy 37.6 TeV averaged over 765 events.
- Fig. 4. The correlation between the derivative of the concentration b and the attenuation lengths of the cascades.
- Fig. 5. The distribution of the main secondary maxima of the ionization curves for the two groups of cascades. Squares are for cascades with $L < 800$ g/cm², crosses - for $L > 800$ g/cm².
- Fig. 6. The cascades distributions for different attenuation lengths in groups with $b < 0$ (solid line) and $b > 0$ (dashed line).
- Fig. 7. The energy dependence of the attenuation lengths obtained from the computer solution of the kinetic equations for different "asymptotic" values (shown by numbers in mb) of the charm production cross sections.
- Fig. 8. The energy dependence of the attenuation lengths from the experiment (circles) and Monte Carlo computer simulations (squares) for all cascades without separating them into two subsamples according to the sign of b .

References

- [1] K. Niu, E. Mikumo, Y. Maeda, *Prog. Theor. Phys.* 46 (1971) 1644.
- [2] S.I. Nikolsky, V.P. Pavlyuchenko, E.L. Feinberg, V.I. Yakovlev, Preprint Lebedev Physical Institute, n. 69, 1975.
- [3] V.S. Aseykin et al, *Izvestia AN SSSR, ser. fiz.*, 38 (1974) 998.
- [4] V.S. Aseykin et al, *Proc. 14 ICRC*, v.7, 2462, Munchen, 1975.
- [5] A.I. Demianov, V.S. Murzin, L.I.Sarycheva, *Yadernye cascadne processy v plotnom veschestve*, Moscow, Izd. Nauka, 1977 (in Russian).
- [6] M. Basile et al, *Lett. Nuovo Cim.* 30 (1981) 487; *Nuovo Cim. A* 65 (1981) 301, 408.
- [7] A. Bodek et al, *Phys. Lett. B* 126 (1983) 499.
- [8] A.Yu. Khodjamiryan, *VANT*, 3(12) (1982) 12.
- [9] L. McLerran, L. Stodolsky, *Phys. Lett. B* 109 (1982) 485.
- [10] R. Hwa, *Phys. Rev. D* 27 (1983) 653.
- [11] K.G. Boreskov, A.B. Kaidalov, *Yad. Fiz.* 37 (1983) 174.
- [12] S.S. Gershtein et al, *Yad. Fiz.* 39 (1984) 60.
- [13] S.I. Nikolsky et al, *Proc. 16 ICRC*, v. 6, 59, Kyoto, 1979.
- [14] V.I. Yakovlev et al, *Proc. 18 ICRC*, v. 5, 102, Bangalore, 1983.
- [15] V.I. Yakovlev, *VANT*, 3(20) (1984) 3.
- [16] I.M. Dremin, V.I. Yakovlev, *Topics on Cosmic Rays, The memorial volumes to the 60-th Anniversary of C.M.G. Lattes*, v. 1, 122, Ed. da Unicamp, Campinas, Brasil, 1984.
- [17] I.M. Dremin, D.T. Madigozhin, V.A. Saakyan, *Yad. Fiz.* 41 (1985) 954; *Izv. AN SSSR, ser. fiz.* 49 (1985) 1271 (*Bull. AS USSR, phys. ser.* 49 (1985) 24).
- [18] I.M. Dremin, V.I. Yakovlev, *Proc. 17 ISMD*, p. 849, Seewinkel, Austria, 1986.
- [19] I.M. Dremin, D.T. Madigozhin, V.I. Yakovlev, *Izv. AN SSSR, ser. fiz.* 50 (1986) 2116 (*Bull. AS USSR, phys. ser.* 50 (1986) 37); *Proc. 19 ICRC*, v. 1, 53, Tbilisi, 1985.
- [20] D.T. Madigozhin, PhD thesis, LPI, Moscow, 1989.
- [21] V.I. Yakovlev, Thesis, LPI, Moscow, 1990.
- [22] Pamir collaboration, *Proc. 20 ICRC*, v. 5, 288, Moscow, 1987.
- [23] I.P. Ivanenko et al, Preprint MSU 91-0402 (1991).

- [24] I.V. Rakobolskaya et al, Nucl. Phys. B 112 (2003) 353c.
- [25] Xin Dong, nucl-ex/0509038.
- [26] J. Adams et al, Phys. Rev. Lett. 94 (2005) 062301.
- [27] A. Tai, J. Phys. G 30 (2004) S809.
- [28] S. Kelly, J. Phys. G 30 (2004) S1189.
- [29] H. Zhang, nucl-ex/0510063.
- [30] M. Cacciari, P. Nason, R. Vogt, hep-ph/0502203.
- [31] R. Vogt, hep-ph/0412303.
- [32] O.I. Piskounova, Preprint Lebedev Physical Institute, n. 118, 1990.
- [33] O.I. Piskounova, N.V. Nikitin, Yad. Fiz. 68 (2005) 1.
- [34] S.P. Baranov, N.P. Zotov, A.V. Lipatov, Yad. Fiz. 67 (2004) 859 (Phys. Atom. Nucl. 67 (2004) 837); hep-ph/0106229.
- [35] I.M. Dremin, D.T. Madigozhin, Yu.N. Vavilov, Kratkie soobcheniya po fizike, LPI, 6 (1988) 9; VANT 5(24) (1988) 153.
- [36] G.T. Zatsepin et al, Izv. AN SSSR, ser. fiz. 58 (1994) 119 (Bull. AS USSR, phys. ser. 58 (1994) 2050); Izv. AN SSSR, ser. fiz. 61 (1997) 559 (Bull. AS USSR, phys. ser. 61 (1997) 440).
- [37] E.V. Bazarov, Preprint Lebedev Physical Institute, n. 102, 1981.
- [38] V.I. Yakovlev, Nucl. Phys. B 136 (2004) 350.
- [39] K. Shinozaki, M. Teshima, Nucl. Phys. B 136 (2004) 18.
- [40] A.A. Ivanov, V.P. Egorova, S.P. Knurenko et al, Izv. RAN 65 (2001) 1221.
- [41] E.S. Nikiforova, JETP Lett. 78 (2003) 757.
- [42] X. Bertou, Proc. 29 ICRC, arg-bertou-X-abs1-he14, Pune, 2005.
- [43] I.M. Dremin, D.T. Madigozhin, V.I. Yakovlev, AIP conf. proc. of 7 Int. Symp. on VHECRI, v. 276, 534, Ann Arbor, 1992.
- [44] L.G. Sveshnikova, O.P. Strogova, Proc. 23 ICRC, v. 4, 33, Dublin, 1993.



ATTENUATION LENGTH $L(E)$, g/cm²

